

Recalibration of damage equivalence factors for fatigue verification of road bridge

Colin Vaccari

EPFL - École Polytechnique fédérale de Lausanne - RESSLab, Lausanne, Switzerland

IST - Instituto Superior Técnico - Lisbon, Portugal

Abstract The current works of revision of the Eurocodes (CEN250 project 2nd Eurocode generation), is an opportunity to update the simplified method (lambda factor method) for fatigue verification for road bridges. Especially as this method is based on old traffic models, it is necessary to establish an update consistent with current European road traffic. This thesis focuses on the λ_{max} verification factor. The aim is to be able to determine new λ_{max} curves using modern traffic models that are more reliable compared to current trends. In addition to this, an improvement is to be made to cover a larger number of cases, both in terms of influence lines and span lengths. The objective remains to propose new λ_{max} curves taking into account the current European traffic observed in order to best monitor the behaviour of road bridges. Several types of traffic were used in order to have an overview and to be able to make a comparison between different models and especially WIM traffic measurements. In conclusion, a new proposal adapted for the verification method with lambda factors is presented. This proposal takes into account the results of the different numerical simulations that could have been performed for a large variety of static systems and various traffic types.

1 Introduction

1.1 Motivation

Fatigue is a key issue in the design and verification of road bridges. Repeatedly changing traffic loads can have a negative impact on the durability of structures. The lambda curves in the current standards need to be revised to be in line with the current European traffic. Indeed, the European standards are based on 30 year old traffic models which are not necessarily representative of current trends. It is therefore required to evaluate and update the lambda values defined in the current standards. The aim of the thesis is to pursue the work on the recalibration of the lambda factors, focusing in particular on the λ_{max} verification factor. For this purpose, current European traffic is evaluated through numerical simulations to determine the λ_{max} factor. In order to assess present traffic, the use of Weight in Motion measurements is part of the development of the new λ_{max} curves. This allows a variety of European road traffic to be assessed and compared with the fatigue models described in the standards.

2 Basic concepts of fatigue design

The fatigue phenomenon occurs when a member is subjected to repeated cycling loadings such as road traffic. This phenomenon is part of the main causes of damages in steel

structures, together with corrosion and wear. Fatigue damage is manifested by the propagation of cracks and results in a loss of resistance over time. It rarely occurs in base materials, but rather in assemblies, which remain the critical location when fatigue loading is checked. It has been demonstrated that geometrical changes, discontinuities and stress concentrations affect the formation and propagation of cracks.

The combined effect of anomalies and stress concentrations can be the source of fatigue crack formation and propagation, even if the applied stresses remain well below the yield point. This crack propagation can lead to yielding or brittle failure. For this reason, the design and fabrication of a structure subjected to repeated variable loads must be done with care in the design and fabrication of the elements and construction details, in order to avoid brittle failure.

2.1 Fatigue strength curve

In order to know the fatigue resistance of steel structures, standardised resistance curves have been established in European construction standards on the basis of a large number of tests. The results are represented in a diagram in which we find, on the y-axis, the stress range $[\Delta\sigma_R]$ and, on the x-axis, the number of cycles [N] observed until failure. These curves can be seen in figure 2.1, according to the detail category.

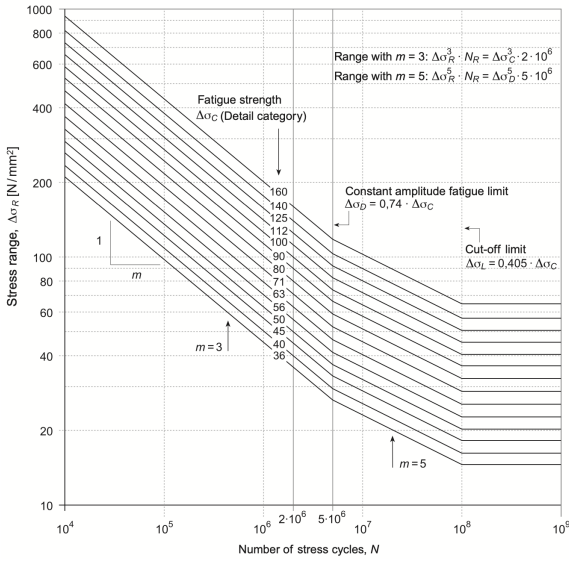


Figure 2.1. Fatigue resistance according to the detail category | m=3, k=5, (extracted from [5])

The resistance curves are each defined by their reference value $\Delta\sigma_C$ which corresponds to $2 \cdot 10^6$ cycles. This value indicates that a detail with this resistance resists a stress range equal to $\Delta\sigma_C$ during $2 \cdot 10^6$ cycles until failure. The constant amplitude fatigue limit, $\Delta\sigma_D$, is where the slope of the curve changes from m to k and corresponds to $5 \cdot 10^6$ cycles. The truncation limit, which corresponds to $1 \cdot 10^8$ cycles, represents the limit below which the effect of stresses can be neglected. The type of detail are classified according to the type of connections and their geometry, such an example is represented in figure 2.2.

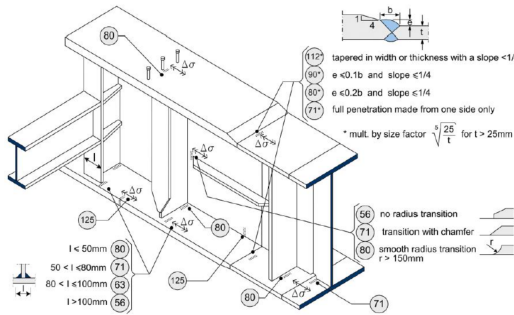


Figure 2.2. common FAT detail categories for steel structures assemblies, (extracted from [3])

2.2 Fatigue safety verification

Fatigue verification is a complementary verification to structural safety check, which can be done in a similar way. the fatigue safety can be verified with 3 different methods.

2.2.1 Verification with the fatigue limit

The first verification remains the simplest and most conservative. This method only considers the maximum stress range. On the basis of tests, it has been shown that the ser-

vice life of a construction detail tends towards infinity when the stress histogram remains below the fatigue limit $\Delta\sigma_D$.

$$\gamma_{Ff} \cdot \Delta\sigma_{i,max} \leq \frac{\Delta\sigma_D}{\gamma_{Mf}} \quad (1)$$

where $\Delta\sigma_{i,max}$ =maximum stress range; $\Delta\sigma_D$ =constant amplitude fatigue limit (CAFL); γ_{Ff} and γ_{Mf} are partial load and resistance factors.

2.2.2 Verification with the cumulative damage

The cumulative damage method allows to consider the whole stress histogram, instead of the maximum stress range. The damage accumulation is expressed:

$$D_{tot} = \sum_{i=1}^k n_i \cdot d_i \quad (2)$$

D_{tot} =Total Damage; n_i =number of cycles to stress range $\Delta\sigma_i$; d_i =damage due to single cycle of stress range $\Delta\sigma_i$.

It is possible to compute the equivalent stress range $\Delta\sigma_{E,2}$, which correspond to $2 \cdot 10^6$ cycles, from the cumulative damage which is a sort of weighting of all the stress ranges of the histogram. The following relationship can then be used (where $\Delta\sigma_c$ =the fatigue resistance of the detail):

$$\gamma_{Ff} \cdot \Delta\sigma_{E,2} \leq \frac{\Delta\sigma_c}{\gamma_{Mf}} \quad (3)$$

2.2.3 Verification with the lambda factor

Since cumulative damage method requires a large number of calculations, a simplified verification method has been established to carry out a fast and efficient calculation while satisfying fatigue safety. The fatigue action effect is determined by the combination of the lambda correction factor and the calculated stress range produce the Fatigue Load Model 3.

$$\Delta\sigma_{Ed,2} = \lambda \cdot \gamma_{Ff} \cdot \Delta\sigma(Q_{fat}) \leq \frac{\Delta\sigma_c}{\gamma_{Mf}} \quad (4)$$

where λ =correction factor; $\Delta\sigma(Q_{fat})$ = stress range according to FLM3. The Fatigue Load Model 3 consists of two 4-axle lorries based on damage equivalent loads from Auxerre traffic measurements from 1986. However a single model cannot precisely represents the total damage due to a whole stress histogram issued from real traffic solicitations. Therefore the lambda correction factor is needed to calibrate the equivalent stress range for real traffic contributions.

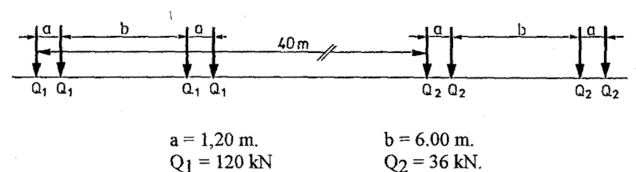


Figure 2.3. Fatigue Load Model 3, (extracted from [13])

2.3 The λ correction factor

The λ factor consists of 4 partial correction factors :

$$\lambda = \lambda_1 \cdot \lambda_2 \cdot \lambda_3 \cdot \lambda_4 \quad \text{but} \quad \lambda \leq \lambda_{max} \quad (5)$$

2.3.1 λ_1 - Damage effect of traffic

The λ_1 factor represents the effect of traffic on the damage as a function of the equivalent span length.

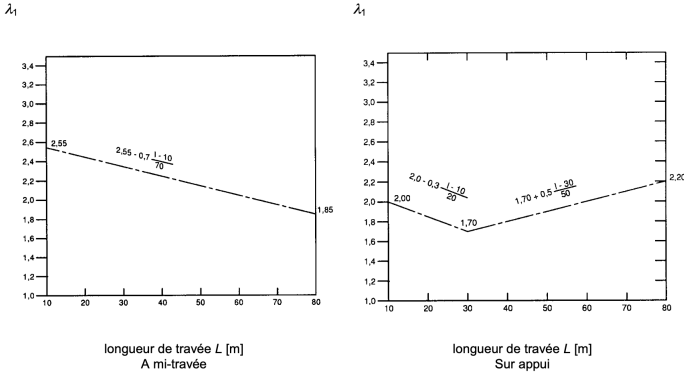


Figure 2.4. λ_1 for moment in road bridges, (extracted from [20])

2.3.2 λ_2 - Traffic volume

The λ_2 factor considers the volume of traffic.

$$\lambda_2 = \frac{Q_{m1}}{Q_0} \cdot \left[\frac{N_{obs}}{N_0} \right]^{1/m} \quad (6)$$

Where Q_{m1} =average gross weight of the lorries in the slow lane; Q_0 =average gross weight of the model; N_0 =number of lorries per year of the model; N_{obs} =number of lorries in the slow lane; m =slope of the Wöhler curve.

2.3.3 λ_3 - Design life

The λ_3 factor takes into account the design life of the bridge, in comparison to the standard design life of 100 years.

$$\lambda_3 = \left[\frac{t_{Ld}}{t_{ref}} \right]^{1/m} \quad (7)$$

t_{Ld} =design life of the bridge; t_{ref} =standard design life

2.3.4 λ_4 - Traffic on other lanes

In the case where there are several lanes of traffic on the road bridge, the factor λ_4 considers the traffic on the other lanes and thus the transverse distribution of stresses.

$$\lambda_4 = \left[1 + \frac{N_2}{N_1} \left(\frac{\eta_2 Q_{m2}}{\eta_1 Q_{m1}} \right)^m + \dots + \frac{N_j}{N_1} \left(\frac{\eta_k Q_{mj}}{\eta_1 Q_{m1}} \right)^m \right]^{1/m} \quad (8)$$

j =number of lane subjected to heavy traffic; N_j =number of lorries per year on lane j ;

2.3.5 λ_{max} - Upper limit

The λ_{max} factor is the upper limit taking account of the fatigue limit. The values of λ_{max} are defined in Eurocode EN 1993-2 [20] in a similar way to the λ_1 factor for equivalent spans ranging from 10m to 80m.

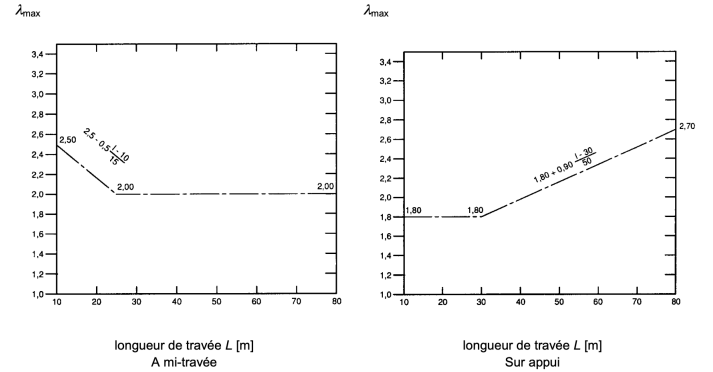


Figure 2.5. λ_{max} for bending moment in road bridges, (extracted from [20])

3 λ_{max} factor determination

The λ_{max} factor is an upper limit that the λ factor can take. This factor is intended to be a limit value that ensure "infinite life" of the considered element subjected to fatigue loads. λ_{max} is function of the maximum loads that can occur over the service life of an element. To ensure, as it is called, an "infinite life", the maximum stress ranges must remain under the constant amplitude fatigue limit (CAFL). In this case, it is assumed that the greatest stress cycles will not result in a crack initiation and therefore ensure a great safety over time.

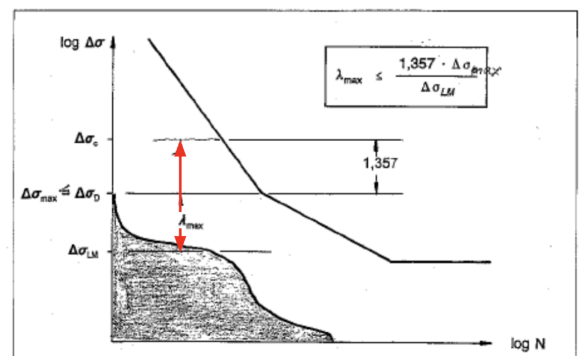


Figure 3.1. Determination of λ_{max} , (adapted from [8])

The category of resistance required to ensure that the maximum stress range remains under the CAFL can be determined with the stress histogram obtained for a real traffic model. λ_{max} is the ratio between the category $\Delta\sigma_C$ and the stress range $\Delta\sigma_{LM}$ issued from the fatigue load model.

$$\lambda_{max} = \frac{\Delta\sigma_C}{\Delta\sigma_{LM}} \geq 1.357 \cdot \frac{\Delta\sigma_{max}}{\Delta\sigma_{LM}} \quad (9)$$

3.1 Sedlacek and Merzenich, 1995

Current λ_{max} curves in EN 1993-2 [20], were introduced based on Sedlacek and Merzenich's work. The numerical simulations date from 1995 [10]. At the time, only a very few influence lines were performed. The traffic model was based on Auxerre traffic measurements. However, the traffic used was generated with a fixed inter-vehicle distance and only flowing traffic. The simulations need to be updated to cover more possibilities in terms of span length and influence lines and to fit with modern traffic.

3.1.1 Traffic Model

The simulations of Sedlacek and Merzenich used the Auxerre traffic data which was considered to be the heaviest traffic in Europe. As explained in [8], Auxerre has been chosen as the reference location for many reasons. The composition of the traffic was intended to corresponds to the estimate future trends, the portion of lorries in the traffic in slow lane was of 32% which was rather high, portion of loaded lorries was 66% which is very efficient and fully documented data were available on a large time period. The traffic analysis made it possible to isolate 4 representative lorry types.

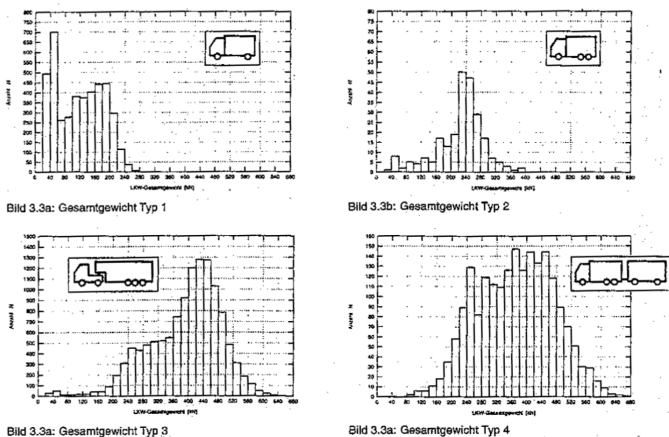


Figure 3.2. Auxerre model - Distribution of vehicle weight, (extracted from [8])

The weights distribution were then approximates by normal distributions for empty and fully-loaded vehicles, which made it possible to generate traffic according to the real composition of traffic.

		Mittelwert der Fahrzeuggewichte $\bar{\sigma}$		Standardabweichung der Fahrzeuggewichte σ_{σ}		Auftrittshäufigkeit f	
		[kN]		[kN]		[%]	
		Spur 1	Spur 2	Spur 1	Spur 2	Spur 1	Spur 2
Klasse 1	LLKW	74	64	31	29	13,3	17,2
	SLKW	183	195	23	28	9,4	10,4
Klasse 2	LLKW	123	107	40	39	0,3	1,3
	SLKW	251	257	31	35	1,0	2,2
Klasse 3	LLKW	265	220	51	68	17,1	28,0
	SLKW	440	463	42	65	48,1	30,4
Klasse 4	LLKW	254	196	37	60	3,6	4,1
	SLKW	429	443	55	64	7,2	6,4
$\Sigma = 100\%$							

Figure 3.3. Statistical data of lorry traffic at Auxerre after filtering out dynamic effects, (extracted from [8])

3.1.2 Comparison with Sedlacek and Merzenich simulations

Being aware of the traffic model that was used in Sedlacek and Merzenich's simulations, it has been possible to use the same model and parameters of traffic to confirm the results provide in the previous numerical simulations and to confirm the validity of our algorithm.

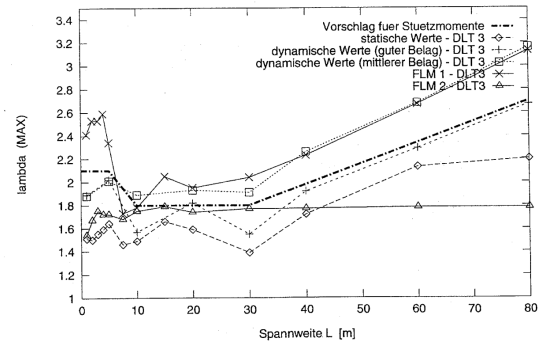


Figure 3.4. Sedlacek and Merzenich Results

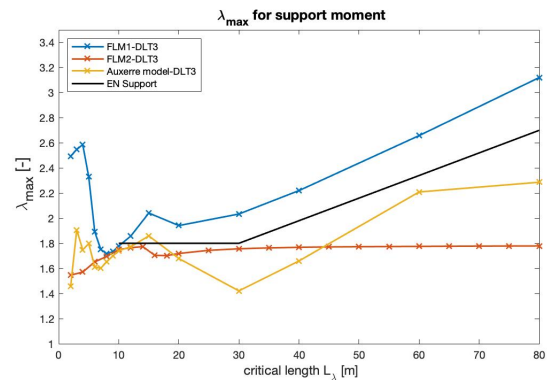


Figure 3.5. Implemented code Results

3.2 λ_{max} criterion

Originally the criterion, for Sedlacek and Merzenich, was that the constant amplitude fatigue limit was set at the level of the maximum stress range $\Delta\sigma_{max}$. This was to ensure sufficient safety to structures check by assuming that the stress ranges were all below the constant amplitude fatigue limit and therefore did not cause damage that would cause the structure to collapse. This criterion especially limits the potential for crack initiation as all the stress ranges are limited by the constant amplitude fatigue limit. This criterion is very sensitive to the traffic parameters since it only considers the maximum stress range. This can differ greatly from one traffic to another, and even within a single traffic depending on the time scale used. The criterion appears to be very safe since by lowering the stress spectrum below the constant amplitude fatigue limit, the damage caused can become very low. Very little damage would mean that one could end up with many cases of over-strength design. This criterion does not seem applicable when using real traffic. Especially due

to the fact that the maximum loads can become very high while in the load models characteristic values are chosen. Moreover, these values will vary greatly depending on the time period used. The criterion has also been adapted to accept the exceedance of which would produce a damage contribution of less than 1% of the total damage.

3.2.1 Adopted criterion

The criterion, proposed by Sedlacek in [13], of 1% exceedance of the total damage is less sensitive to the occurrence of maximum loads. This means that the stress ranges above the constant amplitude fatigue limit produces less than 1% of the total damage. However, that does not guarantee that the total damage due to the stress histogram will remain below 1.0. The effect of this criterion on the results of λ_{max} is also very different depending on the span length. The figure 3.6 represent the total damage when computing λ_{max} with an acceptance of 1% relative damage.

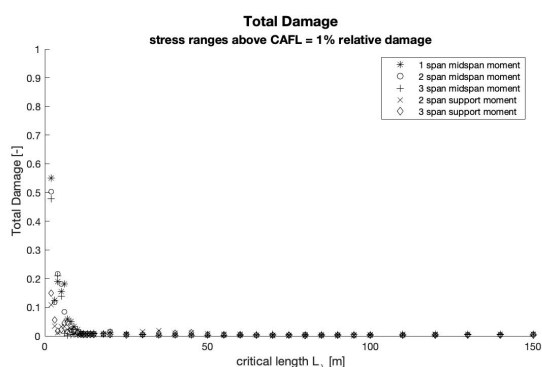


Figure 3.6. Total Damage when determining λ_{max} with 1% relative damage above CAFL

For spans longer than 20 meters, this criterion become very difficult to reach because the total damage is already very small (approximately 0.001). To use a more appropriate criterion, it is proposed to allow an absolute damage of 0.01 for stress ranges above the CAFL while ensuring that the total damage remains below 1.0. In comparison with the previous figure, the figure 3.7 represent the total damage when computing λ_{max} with this criterion.

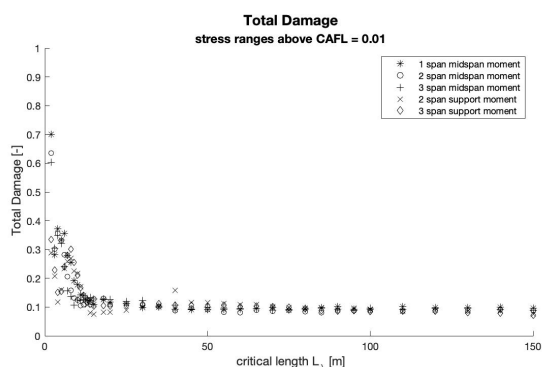


Figure 3.7. Total Damage when determining λ_{max} with 1% relative damage above CAFL

The results of the total damage are still widely below the limit of 1.0 which is important to satisfy. otherwise the criterion would not be applicable because it would not be safe, let alone to satisfy an "infinite" service life. For longer spans, the total damage is approximately equals to 0.1 which is still safe. It will result in reducing the values of λ_{max} and generate more economic designs than those that could happen when using the previous criterion.

4 λ_{max} calibration procedure

The procedure to determine λ_{max} is very similar to the procedure used to obtain λ_1 . Therefore, the algorithm implemented was adapted from the Master thesis of Gianluca Bianchi [3].

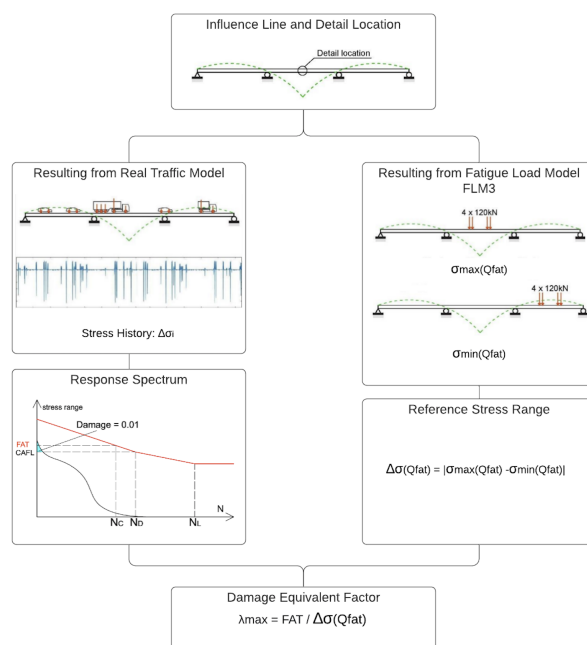


Figure 4.1. λ_{max} factor computation procedure

The method allows the calibration of the factor by comparing a real traffic model with the FLM3 model described in the Eurocode for the fatigue design of road bridges. The fatigue load calculation from the FLM3 model is performed, and a cumulative damage calculation is used for the real traffic model. In contrast to the λ_1 calculation. Here the resistance curve is adjusted to find a damage equals to 0.01 for stress ranges located above the constant amplitude fatigue limit. Then, λ_{max} is the ratio between the resistance of the strength curve and the reference stress range $\Delta\sigma_{Qfat}$.

4.1 Influence lines

In order to have a good overview and to propose new λ_{max} curves that considers a large number of influence lines, the simulations carried out for the λ_{max} calculations use 5 static configurations presented below.

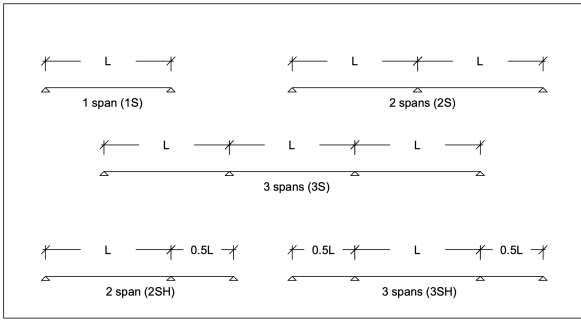


Figure 4.2. Static systems for the recalibration of λ_{max}

Various influence lines were added, including support reactions and mid-span moments on the end spans. Moreover, 2 influence lines such as intermediate moment and intermediate shear evaluate the respective forces for a section located at $0.15 \cdot L$ from the support, which is currently the limit between span and support sections. A total of 44 influence lines were performed.

4.2 Fatigue Load Model 3

The load model prescribed by the Eurocode is the Fatigue Load Model 3. This consists of 2 equivalent lorries that can act on the influence line. Depending on the length of the influence line, the second lorry must be introduced to calculate the fatigue stress range $\Delta\sigma_{Qfat}$. The only condition to complete is the minimum distance of 40 meters between the 2 vehicles (see fig. 2.3). The use of a second lorry considerably increases the possibility of mistakes when calculating $\Delta\sigma_{max}$. This is due to the positioning of the second lorry as it is not fixed. For the recalibration of the λ factors, it was therefore decided to use only the first FLM3 lorry. This simplification will avoid possible mistakes and will clarify any doubts that may be present when using the FLM3 model. Although the second FLM3 lorry was introduced for obvious reasons (explained in section 2) in order to best match the real traffic behaviour for every influence lines. The use of only one truck will not change the veracity of the results as this difference will be directly considered in the calibration of the lambda factors.

4.3 Weight In Motion (WIM)

WIM measuring stations provide real traffic data and are nowadays the standard for traffic load measurements. These data can be used directly to calibrate the lambda factors, which makes it possible to be in line with current European traffic. They provides useful informations such as axles load, inter-vehicle distance, inter-axles distance and speed. They also indicates the traffic intensity and helps deriving the annual traffic flow. The various WIM traffic used for the recalibration are taken from 6 different WIM stations, located in Switzerland, Sweden and in the Netherlands.

4.3.1 Comparison of the WIM database

The simulations use the 6 available WIMs. These WIMs have different and various traffic parameters and will be useful to determine a new λ_{max} curve that will include the traffic diversity. The following table compare some key parameters of the different WIMs.

	Average weight of lorries Q_{m1} [kN]	Average weight of axles Q_{ma} [kN]	Average vehicle distance [m]	Nobs [-]	Traffic type
A16, NL	349.28	75.81	255.24	2'100'000	long distance
Sweden	402.85	74.98	1019.79	400'000	long distance
Löddeköpinge, SE	366.25	71.23	1077.66	500'000	long distance
Gotthard, CH	307.67	73.02	423.83	400'000	long distance
Ceneri, CH	280.17	69.63	482.73	675'000	medium/long distance
Denges, CH	250.58	67.63	2191.10	500'000	medium distance

Figure 4.3. WIM characteristics

The traffic characteristics are quite different, which makes it possible to have a good diversity of traffic between very heavy and very dense European traffic such as the A16 and lighter traffic such as that present in Switzerland. All these different data will allow to evaluate if λ_{max} results are linked to these parameters and to propose λ_{max} curves based on various European road traffics.

4.3.2 Choice of WIM measurements as the real traffic model for λ_{max} determination

The real traffic model used in the numerical simulations could be derived from different models such as Fatigue Load Model 4, Auxerre model described in [8], or in this case with WIM stations. The choice to use WIM traffic is motivated by the use of modern traffic measures. It also allows to consider the traffic in his entirety, considering also extreme load value that could affect the initiation and propagation of cracks. Indeed, Traffic model are more intended to represent average traffic value, it is therefore complicated to use them as reference when calculating factor as λ_{max} , which is mainly governed by maximum stress values. It was also difficult to find acceptable results with the use of traffic models, especially as the stress histogram was very condensed and did not allow the 1% absolute damage criterion to be reached precisely.

4.4 Dynamic amplification factor

Dynamic effects can obviously have an influence when calculating and determining road traffic effects. It is not easy to describe dynamic effects because they depend on many parameters. As referring to road bridges, it is then necessary to determine the behaviour due to the interaction between the structure and the passage of vehicles. There are three main parameters to be considered, namely the dynamic properties of the vehicle, the response of the bridge and the contact surface. Dynamic amplification factors are calculated for special cases. In reality, high dynamic effects are quite rare

and do not necessarily coincide with the highest load cases. It is therefore not easy to find a realistic factor that does not overestimate the dynamic effects, especially when calculating the λ curves. In reality to adjust the stress histogram, it has been shown in [14] that an additional dynamic amplification factor between 1.0 and 1.05 was sufficient to estimate the real dynamic effects.

5 Analysis of the results

5.1 Final parameters for the λ_{max} curves

The final simulations for the λ_{max} factor are set with the following parameters:

- Fatigue strength curve slope: $m|k=3|5$
- Fatigue Load Model: FLM3 with a single lorry of 480 kN, divided in axles
- Bridge design life: 100 years
- Criterion: λ_{max} set for $D_{CAFL} = 0.01$
- Real Traffic Model: WIM measurements (A16-NL, Sweden, Löddekoping, Ceneri, Gotthard, Denges) without dynamic amplification factor
- Heavy vehicles per year: annual heavy vehicles observed for each traffic
- Inter-vehicles distance: measured distances extracted from WIM measurements
- span length: ranging from 0 to 200m

Classification The results obtained for the influence lines are checked and processed. Firstly, the results are checked to be acceptable according to the following two conditions: the damage above the constant amplitude fatigue limit must be equal to $D=0.01$ with a tolerance of 3%, and the total damage must be smaller than or equal to 1.0.

$$0.0097 \leq D_{CAFL} \leq 0.0103 \quad (10)$$

$$D_{tot} \leq 1.0 \quad (11)$$

Then the values that satisfy these 2 conditions are kept and a linear interpolation is carried out on the basis of these values. The interpolation is performed meter by meter for span lengths ranging from 10m to 200m. The influence lines are then classified into 4 groups; mid-span bending moment, support bending moment, mid-span shear, support shear.

5.2 λ_{max} results comparison

When the results are put together, the same trend is observed for λ_{max} , but it can be observed that some shifts between the various WIM results. As an example, the comparison is shown in fig. 5.1 for the mid-span bending moments.

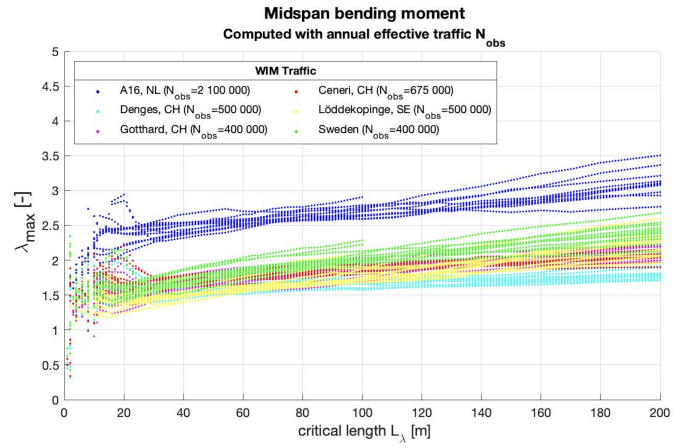


Figure 5.1. λ_{max} comparison for WIM measurements

λ_{max} values are much higher for the WIM traffic from the A16 in the Netherlands. However, the curves have a rather similar behaviour. The results seem to be influenced by the annual number of heavy vehicles. It is then proposed to correct the results following a factor derived from the λ_2 . The λ_2 factor as described in EN 1993-2 [20] considers both the annual traffic and average weight of heavy vehicles. However, the average weight of lorries should not greatly influence the results on λ_{max} as it is mainly a function of the maximum values. The proposed adjustment factor λ_2^* is then only a function of the annual number of heavy vehicles.

$$\lambda_2^* = \left[\frac{N_{obs}}{N_0} \right]^{1/5} \quad (12)$$

The value of the lambda correction factor should this time be bounded not by λ_{max} but by $\lambda_{max} \cdot \lambda_2^*$

$$\lambda = \lambda_1 \cdot \lambda_2 \cdot \lambda_3 \cdot \lambda_4 \leq \lambda_{max} \cdot \lambda_2^* \quad (13)$$

5.2.1 λ_{max} corrected results

Now, for the results presented, the correction factor λ_2^* is applied. The figures show the corrections for $N_0 = 500'000$.

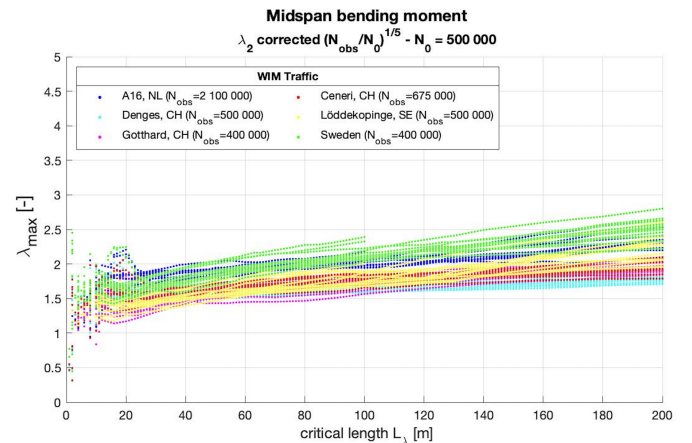


Figure 5.2. λ_{max} results for mid-span moment corrected with $N_0 = 500'000$

The correction seems to work well, as the results are well grouped regardless of the type of traffic. There are of course some small differences, especially between Swiss traffic which is quite light compared to Swedish and Dutch traffic.

5.3 λ_{max} curves proposition

To propose new λ_{max} curves, the WIM results are corrected with the previously determined λ_2^* factor. The curves are interpolated meter by meter, which makes it possible to determine the mean and the standard deviation for each critical length value. For each group of results, the proposed λ_{max} curve is based on the 95% fractiles using approximating curve segments.

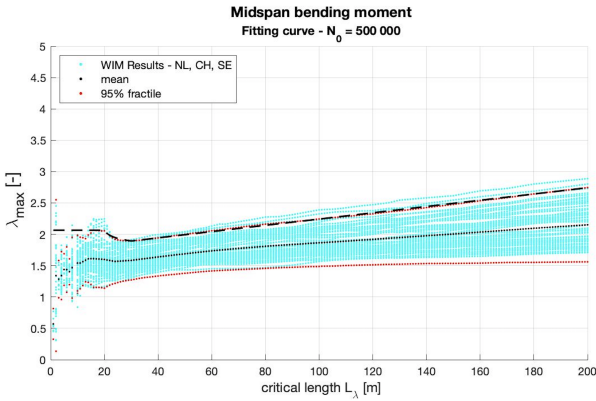


Figure 5.3. λ_{max} fitting curve for mid-span moment corrected with $N_0 = 500'000$

This approach was applied for each group of influence lines. This allowed us to derive λ_{max} curves for the mid-span moment, support moment, mid-span shear and support shear.

5.4 New λ_{max} curves

The final λ_{max} curves presented below are calibrated for an annual number of lorries, as currently defined in the European standard with $N_0 = 500'000$. The curves are all defined for critical lengths L_λ ranging from 5 to 200m. The parametric equations is similar for each influence lines. The curves could then be defined by a unique equations which parameters are defined for each influence lines.

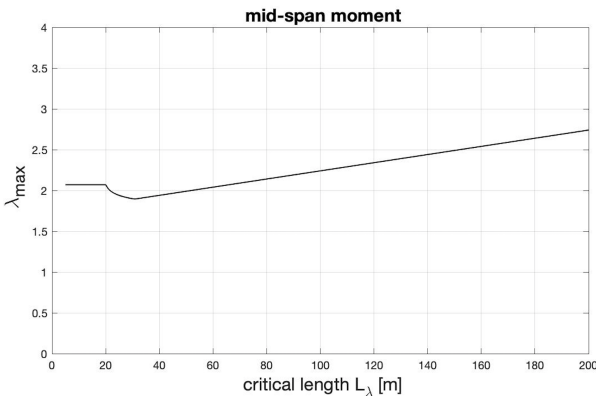


Figure 5.4. λ_{max} final curves mid-span moment

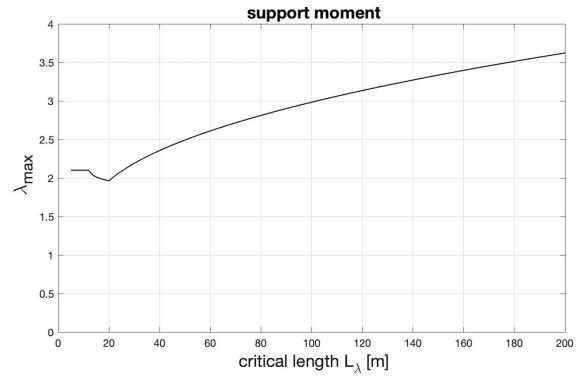


Figure 5.5. λ_{max} final curves support moment

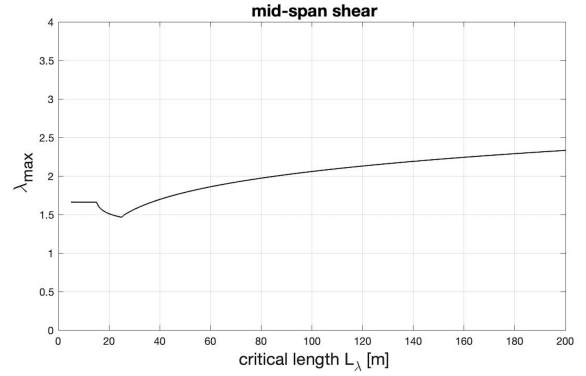


Figure 5.6. λ_{max} final curves mid-span shear

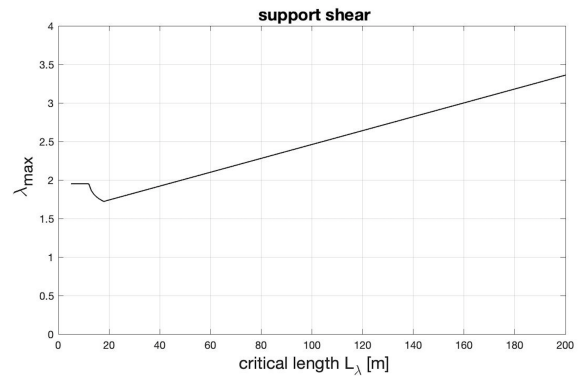


Figure 5.7. λ_{max} final curves support shear

The following figure therefore shows the equation in general form with the parameters to be applied for each curve.

		MM SM MV SV			
L_1		20	12	15	12
L_2		30	20	25	18
A		2.07	2.10	1.66	1.95
B		0.55	0.65	0.55	0.65
C		1.74	1.40	0	1.56
a		0.05	0.045	0.081	0.10
b		-	0.45	0.162	-
c		0.005	0	0	0.009
d		0	0.21	1.00	0

		λ_{max}
$5 \leq L_\lambda \leq L_1$		A
$L_1 \leq L_\lambda \leq L_2$		$B + \frac{(A-B)}{L_\lambda - (L_1 - 1)^a}$
$L_2 \leq L_\lambda \leq 200$		$C + c \cdot L_\lambda + d \cdot (L_\lambda - (L_1 - 1))^b$

Figure 5.8. λ_{max} parametric equation

5.5 Effects of the slopes of the Wöhler curve

All previous results were based on the standard resistance curve with double slope $m|k=3|5$. Other fatigue strength curves with slopes such as; $m=3$; $m=5$; $m|k=5|9$ and $m|k=4|6$ were evaluated. It has been determined that the λ_{max} results always have the same behaviour with a constant gap for all critical length L_λ .

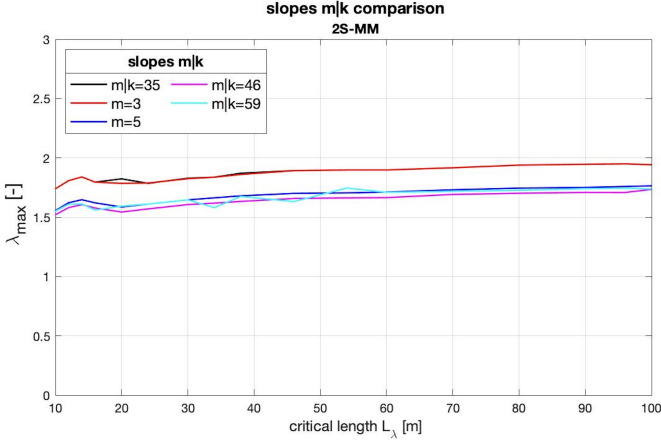


Figure 5.9. λ_{max} comparison for different slopes of the fatigue strength curve

Due to the 1% relative damage criterion used, the difference between the curves is mainly due to the ratio between the constant amplitude fatigue limit (CAFL) and the resistance category $\Delta\sigma_C$. It has then been possible to compute analytically the correction that must be applied when different fatigue strength curves are used.

The λ_{max} curve must therefore be corrected with respect to the slope of the fatigue strength curve in the region between N_C and N_D . In the case where the change in slope of the fatigue strength curve occurs at $N_C = 2$ millions cycles, m must be replaced by k in the equation 14.

$$\lambda_{max(m|k)} = \lambda_{max(3|5)} \cdot \left(\frac{2}{5}\right)^{(m-3)/(m \cdot 3)} \quad (14)$$

6 Conclusion

This work allowed to study in depth the behaviour of the λ_{max} factor used in the simplified fatigue verification method for road bridges. This verification method has to be updated and recalibrated according to the traffic that can be observed on European roads nowadays. Indeed, the lambda factors of this simplified method reflect the difference between the damage caused by the fatigue load model and the damage that would be caused by a real traffic. It is therefore important to carry out this update to ensure that the verification method is consistent and guarantees the safety of the structures using this method. The calibration of the new λ_{max} curves is based on WIM measurements from 6 different stations (lo-

cated in Switzerland, Sweden and in the Netherlands). This allowed to evaluate several types of traffic with parameters that could be very different. To determine the new curves, a new criterion was used. This criterion allows an exceed of 1% of absolute damage for stress ranges above the constant amplitude fatigue limit. It has been shown that this criterion is more adequate and remains safe. The choice to use WIM measurements is explained by the fact that it accounts for real traffic and in particular the extreme values of traffic loads that can occur. In contrast to traffic models, which report average values of heavy vehicles and do not represent the maximum values. In the case of λ_{max} calibration, it seems preferable to use WIM measurements, which allow an evaluation of the traffic in its entirety. WIM data also allows the dynamic effects contained in the measurements to be considered, and it has been shown that WIM measurements do not necessarily require additional dynamic amplification in terms of fatigue. In the simulations done during this project, 44 influence lines were therefore calculated in order to cover a larger number of cases than in previous simulations. The influence lines were also evaluated for span lengths up to 200m. These new numerical simulations allowed the influence lines to be classified into 4 groups; mid-span bending moment, support bending moment, mid-span shear forces and support shear forces. It was therefore possible to determine 4 λ_{max} curves that take into account the 44 influence lines.

6.1 Future works

The numerical simulations are now well developed with a large number of parameters that allow the evaluation of a large number of influence lines with different traffic models, be it FLM4, Auxerre, A16 models, or traffic measurements with the help of WIM stations. Further investigations could be carried out regarding dynamic amplification factors. This would provide confirmation of the assumptions done in this work.

It would be interesting to perform simulations with multi-lanes traffics. Indeed, all the simulations that were carried out in this work only considered a model for a single traffic lane, an adaptation of the algorithm in order to study the effect of 2 traffic lanes for example would be interesting and would allow the study of the λ_4 factor.

In addition, it would be interesting to pursue the work started to apply the λ_1 and λ_{max} results for other fatigue resistance curves. In particular, it would be possible to find results for concrete bridge deck elements. This would allow to complete the current algorithm and to compare these results with the actual curves defined in Eurocode EN-1992-2.

List of Symbols

D_{CAFL}	Damage above CAFL
D_{tot}	Total damage
E_d	Design value of the effects of fatigue actions
L_λ	Critical length
N	Number of cycles
N_j	Number of lorries per year on lane j
N_{obs}	Number of lorries per year on the slow lane
Q_0	Average weight of the model
Q_{fat}	Fatigue Load Model
Q_i	Average weight of the considered lorries
Q_{m1}	Average weight of the lorries in the slow lane
Q_{mj}	Average weight of lorries on lane j
γ_{Ff}	Fatigue action effects safety factor
γ_{Mf}	Fatigue strength safety factor
$\Delta\sigma$	Stress range
$\Delta\sigma_C$	Fatigue strength at 2 millions cycles
$\Delta\sigma_D$	Fatigue strength at 5 million cycles
$\Delta\sigma_L$	Fatigue strength at 100 million cycles
$\Delta\sigma_{E,2}$	Equivalent direct stress range at 2 million cycles
λ	Damage equivalence factor
λ_1	Partial factor for the damage effect of traffic
λ_2	Partial factor for the traffic volume
λ_3	Partial factor for the design life
λ_4	Partial factor for the traffic on other lanes
λ_{max}	Maximum damage equivalent factor

References

- [1] Nariman Maddah, *Fatigue Life Assessment of Roadway Bridges based on Actual Traffic Loads*, EPFL Thèse N°5575, 2013.
- [2] Cláudio Alexandre Pereira Baptista, *Multiaxial and variable amplitude fatigue in steel bridges*, EPFL Thèse N°7044, 2016.
- [3] Gianluca Bianchi, *European traffic on road bridges and recalibration of damage equivalence factor for fatigue verification*, EPFL Master Thesis, 2019
- [4] A. Nussbaumer and S. Wallbridge, *Background for determination of the fatigue load correction factor in SIA codes*, EPFL, 2009
- [5] Manfred A. Hirt, Rolf Bez and Alain Nussbaumer, *Construction Métallique (TGC volume 10)*, PPUR, 2009
- [6] Jean-Paul Lebet and Manfred A. Hirt, *Ponts en acier (TGC volume 12)*, PPUR, 2009
- [7] A. Nussbaumer, J. Oliveira Pedro, C.A. Pereira Baptista and M. Duval, *Fatigue damage factor calibration for long-span cable-stayed bridge decks*, in Structural Integrity, 2019, chapter 7, pp. 369–376
- [8] G. Sedlacek, G. Merzenich, M. Paschen, A. Brules, L.Sanpaolesi, P.Croce, J.A. Calgaro, M. Pratt, Jacob, M. Leendertz, v. de Boer, A. Vrouwenfelder and G. Hanswille, *Background document to EN 1991 - Part 2 - Traffic loads for road bridges - and consequences for the design*, JRC Scientific and Technical Reports, 2008
- [9] P. Croce, *Background to fatigue load models for Eurocode 1: Part 2 Traffic Loads. Progress in Structural Engineering and Materials*, 2001
- [10] G. Merzenich and G. Sedlacek, *Hintergrundbericht zum Eurocode 1 - Teil 3.2: "Verkehrslasten auf Straßenbrücken"*, Forschung Heft Straßenbau und Straßenverkehrstechnik, 1995
- [11] P. Kunz, Manfred A. Hirt, *Grundlagen und Annahmen für den Nachweis der Ermüdungssicherheit in den Tragswerksnormen des SIA*, 1991
- [12] M. Sjaarda, T. Meystre, A. Nussbaumer, Manfred A. Hirt, *system-atic approach to estimating traffic load effects on bridges using weigh- in-motion data*, Stahlbau 89, H. 7, S. 585–598, 2020
- [13] G. Sedlacek, H. Eisel, W. Hensen, B. Kuhn, *Leitfaden Zum DIN-Fachbericht 103 Stahlbrücken*, John Wiley Sons, 2004
- [14] J. Maljaars, *Evaluation of traffic load models for fatigue verification of European road bridges*, Engineering Structures, Volume 225, 2020, 111326, ISSN 0141-0296
- [15] J. Leander, *Reliability evaluation of the Eurocode model for fatigue assessment of steel bridges*, Journal of Constructional Steel Research, Volume 141, 2018, Pages 1-8, ISSN 0143-974X
- [16] J.-A. Calgaro, M. Tschumi, H. Gulvanessian, *Designers' Guide to Eurocode 1: Action on bridges*, 2010
- [17] *SETRA: Eurocodes 3 and 4 - Application to steel-concrete composite road bridges*, Paris, 2007
- [18] *Eurocode 1 - Actions on structures - Part 2: Traffic loads on bridges*, European committee for standardization, 2003
- [19] *Eurocode 2 - Design of concrete structures - Part 2: Concrete bridges*, European committee for standardization, 2005
- [20] *Eurocode 3 - Design of steel structures - Part 2: Steel Bridges*, European committee for standardization, 2006
- [21] *Eurocode 3 - Design of steel structures - Part 1-9: Fatigue*, European committee for standardization, 2005
- [22] *Swiss standard SIA 261 - Actions sur les structures porteuses*, 2014
- [23] *Swiss standard SIA 263 - Construction en acier*, 2013